

# Aerothermodynamic Study of Slender Conical Vehicles

R. A. Thompson,\* E. V. Zoby,†  
K. E. Wurster,‡ and P. A. Gnoffo§  
NASA Langley Research Center, Hampton, Virginia

A study was performed to assess the applicability of some current techniques which can be used for aerothermal predictions over slender spherically blunted cones. Predictions using a viscous-shock-layer method and several engineering approaches were compared with experimental results from flight- and ground-based tests, with each other, and with other detailed results. Good agreement was obtained in comparisons with laminar and turbulent heating data from the Reentry F flight vehicle and with the wind-tunnel data. In particular, the viscous-shock-layer method was shown to yield excellent comparisons and to be useful in providing detailed flowfield and surface values for slender blunted cones. Detailed comparison of the engineering code predictions with the viscous-shock-layer results generally showed good agreement except for the laminar predictions at angle attack on the forward cone surface.

## Nomenclature

EQLB	= equilibrium air
$L$	= length, ft
$M$	= Mach number
$P$	= pressure, lb/ft <sup>2</sup>
$\dot{q}$	= heat-transfer rate, Btu/ft <sup>2</sup> -s
$r_n$	= nose radius, ft
$s$	= surface distance, ft
$x$	= axial distance, ft
$\alpha$	= angle of attack, deg
$\gamma$	= ratio of specific heats
$\theta_c$	= cone half-angle, deg
$\phi$	= circumferential angle measured from windward centerline, deg

## Subscripts

$o$	= stagnation point
$w$	= wall value
$ref$	= reference condition
$\infty$	= freestream value

## Introduction

RECENT interest in hypersonic vehicles has increased the need for verification and application of aerothermal prediction techniques in many areas. These prediction techniques are useful for design studies, and they can aid in developing improved methodology for extrapolating wind-tunnel data to flight conditions. However, before any method can be used with confidence, it must be verified as accurately as possible. This is especially true if future mission goals are so demanding that excessive conservatism applied to computational predictions (or experimental data) will inhibit the successful design of these vehicles.

The present paper addresses the verification and application of aerothermal prediction techniques which may be useful in such design studies. A primary purpose of this paper is to

demonstrate the applicability of several computer codes which can be used for high-speed flowfield and aerodynamic heating predictions over slender bodies. The codes considered in detail herein range in complexity from "engineering" formulations<sup>1-3</sup> to finite-difference solution of the viscous-shock-layer (VSL) equations.<sup>4-6</sup> In general terms, the engineering programs employ various levels of approximation in determining surface pressure, heat transfer, and real gas effects. They are typically used for conceptual design because they are quick running and can be used for extensive parametric studies. The VSL method is also useful for studies of generic body shapes and can provide detailed information such as surface heat transfer and pressure distributions, force-and-moment values at small angles of attack (where flow is attached in circumferential direction), and shock-layer properties.

To demonstrate the applicability of these codes, the results of heating predictions are compared with flight<sup>7</sup> and ground test data,<sup>8,9</sup> with each other, and with another detailed method.<sup>10</sup> This combination of data comparisons provides a sound procedure for verification of prediction methods and serves to illustrate potential errors or problems.

## Computational Methods

### Engineering Codes

The MINIVER program<sup>1</sup> is an engineering code that can be easily used in computer-aided design systems such as AVID.<sup>11</sup> The code provides the user with a menu for selection of methods to compute postshock and local flow properties as well as heating-rate values. The stagnation-point heating is computed with the Fay-Riddell<sup>12</sup> method; the local laminar values are computed by the Blasius<sup>13</sup> skin-friction method and a modified Reynolds analogy with Eckert reference enthalpy<sup>14</sup> to account for compressibility effects; and the turbulent levels can be computed by the Shultz-Grunow<sup>15</sup> skin-friction technique with reference enthalpy and a Reynolds analogy or with the Spalding-Chi<sup>16</sup> skin-friction method and a Reynolds analogy form. In addition, several boundary-layer transition criteria are provided as well as methods to compute the heating over the transitional flow regime (continuum to free molecule) and for swept cylinder and interference heating conditions. The calculations can be based on perfect gas or equilibrium air chemistry. The flow can be computed for two-dimensional or axisymmetric surfaces with angle-of-attack effects simulated by a tangent-cone or an approximate crossflow option. Axisymmetric effects are available only through use of the Mangler<sup>17</sup> transformation for flat plate to sharp cone conditions. This option does not permit the user to study bluntness effects, since the axisymmetric effects are treated as a constant. Also, the code does not provide any method to account for

Presented as Paper 87-1475 at the AIAA 22nd Thermophysics Conference, Honolulu, HI, June 8-10, 1987; received March 28, 1988; revision received Dec. 20, 1988. Copyright © 1989 American Institute of Aeronautics and Astronautics, Inc. No copyright is asserted in the United States under Title 17, U.S. Code. The U.S. Government has a royalty-free license to exercise all rights under the copyright claimed herein for Governmental purposes. All other rights are reserved by the copyright owner.

\*Aerospace Technologist, Aerothermodynamics Branch, Space Systems Division. Member AIAA.

†Aerospace Technologist, Aerothermodynamics Branch, Space Systems Division. Associate Fellow AIAA.

‡Aerospace Technologist, Vehicle Analysis Branch, Space Systems Division. Member AIAA.

§Aerospace Technologist, Aerothermodynamics Branch, Space Systems Division. Senior Member AIAA.

the pressure overexpansion or variable entropy effects on heat transfer along blunted vehicles.

Another technique, due to DeJarnette and Hamilton,<sup>2</sup> uses the axisymmetric analog concept<sup>18</sup> which has been applied extensively<sup>19,20</sup> to heating-rate calculations over three-dimensional bodies. This method is used in the aerospace industry and is referred to as NHEAT or AEROHEAT. For application of the axisymmetric analog concept, the three-dimensional boundary-layer equations are written in the streamline coordinate system, and the crossflow velocity (tangent to the surface and normal to the streamline direction) is assumed to be zero. The resulting equations are identical to the axisymmetric zero degree angle-of-attack forms if the distance along the streamline is considered the surface distance and the metric representing the streamline spreading is equated to the axisymmetric body radius. Several techniques<sup>19,21</sup> have been employed by DeJarnette and associates for computing the inviscid surface streamline paths and the metric coefficients associated with the spreading. The basic Maslen<sup>22</sup> method is used to compute the shock shape corresponding to each inviscid surface streamline, and mass balancing is used to account for local entropy effects on the surface heating. The approximate methods of Cohen<sup>23</sup> are used to compute the stagnation-point and local laminar heating values. Several turbulent heating methods are also included. Local pressures are computed analytically or can be input, and the gas properties can be computed by perfect gas or equilibrium air assumptions.

The INCHES code<sup>3</sup> is an approximate inviscid plus boundary-layer method that was initially developed for engineering calculations of radiation and convective heating rates for planetary missions. The code uses a modified Maslen technique<sup>24</sup> and computes the axisymmetric zero degree angle-of-attack flowfield over paraboloids, ellipsoids, hyperboloids, and sphere cones. Since the code computes the flowfield over the desired body rather than the inverse method suggested by Maslen, a better definition of inviscid properties is obtained. For example, the code computes the overexpansion and recompression of the pressure for blunted cones. Variable entropy can be included by using local inviscid properties located a boundary-layer thickness away from the body surface. The code uses the Cohen stagnation-point heating method and a Blasius skin-friction coefficient based on momentum thickness with Eckert reference enthalpy and a modified Reynolds analogy to compute local laminar heating. The turbulent heating equations also employ a skin friction based on momentum thickness. The exponent on the Reynolds number is computed with the velocity profile exponent as a function of the momentum-thickness Reynolds number. A recent study<sup>3</sup> included angle-of-attack effects (crossflow) in the heating calculations over the windward and leeward symmetry planes of sphere cones through use of the DeJarnette and Davis<sup>19</sup> method. However, the inviscid shock shape and flowfield at angle of attack are computed based on the equivalent cone. The variable exponent for the momentum-thickness Reynolds number is based on experimental data<sup>25</sup> measured in axisymmetric nozzles.

#### Viscous-Shock-Layer Code

The three-dimensional viscous-shock-layer method is based on the solution of a subset of the Navier-Stokes equations in which parabolic approximations are made in both the streamwise and crossflow directions. In the VSL method, the entire shock layer is modeled with a single set of equations which are valid through the inviscid and viscous regions and thereby eliminate inherent difficulties encountered in matching boundary-layer and inviscid solutions, e.g., accounting for entropy effects. Davis<sup>26</sup> developed the application of the viscous-shock-layer equations for two-dimensional flows over axisymmetric configurations. Murray and Lewis<sup>4</sup> extended the method to three dimensions and applied their code (VSL3D)

to spherically blunted conical configurations. Later, Thareja et al.<sup>5</sup> modified the VSL3D code to include transition and turbulent flow and the capability for treating air in chemical equilibrium. A further extension of the code was made by Swaminathan et al.<sup>6</sup> wherein the chemistry modeling was changed to treat chemical nonequilibrium in the shock layer.

Turbulence modeling in the VSL3D code is achieved using an algebraic eddy-viscosity model. This two-layer turbulence model accounts for pressure gradients<sup>27</sup> and three-dimensional effects in the inner layer.<sup>28</sup> The outer layer model is that given by Clauser<sup>29</sup> and Klebanoff.<sup>30</sup> During transition to turbulence, the composite eddy viscosity is modified using the Dhawan and Narashima method.<sup>31</sup> Thermodynamic and transport properties for equilibrium air calculations with the VSL3D code were obtained from Hansen.<sup>32</sup>

## Experimental Data

### Reentry F Flight Test

One purpose of the present paper is to draw attention to available experimental data which can be used for code comparison and verification. Most notable of the data presented in this paper are laminar, transitional, and turbulent heating data measured on a slender conical body during free flight.<sup>7</sup> This flight experiment, known as Reentry F, was performed in 1968 to provide accurate measurement of turbulent heating rates on a nearly sharp conical vehicle in regions where Mach number, Reynolds number, freestream enthalpy, and ratios of wall-to-total temperature could not be obtained by ground-based experiments. The Reentry F vehicle was a 5-deg sphere cone, 13 ft in length with an initial nose radius of 0.1 in. A graphite nosetip extended for the first 7.69 in. followed by a conical beryllium frustrum. Temperature measurements were obtained for the prime data period at altitudes between 120,000 and 60,000 ft at freestream Mach numbers near 20. These temperature data were reduced to heating rates and compared with prediction techniques existing at that time. In addition, the measurements provided experimental information<sup>33</sup> on hypersonic boundary-layer transition in the flight environment. These data hold importance today since they are useful for comparison with prediction techniques, and practical application of transition criteria continues to be of primary importance.

### Wind-Tunnel Data

Many sources of hypersonic wind-tunnel heat-transfer data over blunted conical bodies are available in the open literature. For this paper, the ground test data presented in Refs. 8 and 9 were used for comparison. The data of Ref. 8 include both laminar and turbulent heat transfer for an 8-deg sphere cone under perfect gas, relatively low Mach number conditions. In Ref. 9, laminar heat-transfer data for a blunted 15-deg cone in perfect gas, Mach 10.6 flow were obtained and are compared with VSL3D predictions to illustrate angle-of-attack capability.

## Results and Discussion

In this section, comparative analyses of the VSL3D and engineering code predictions with experimental data, other computational results, and each other are presented and discussed. Actual heating rates for most of these cases have been normalized with a reference heating rate, but the relative comparisons are unchanged.

### Comparison of Detailed Prediction Methods

One step in the verification of prediction methods is the comparison of results obtained with different codes. For this paper, specific comparisons of heating rates obtained with VSL3D and a parabolized Navier-Stokes (PNS) code<sup>10</sup> were

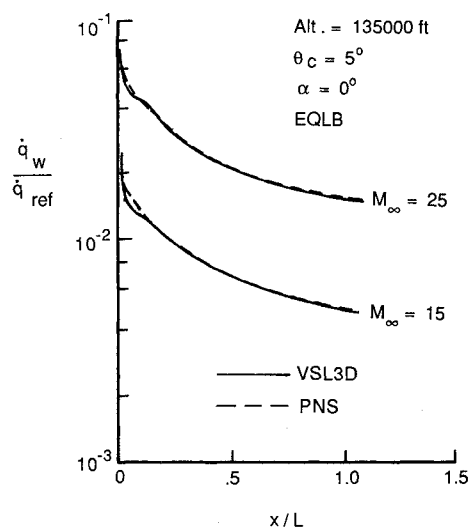


Fig. 1 Comparison of heating predictions from detailed codes.

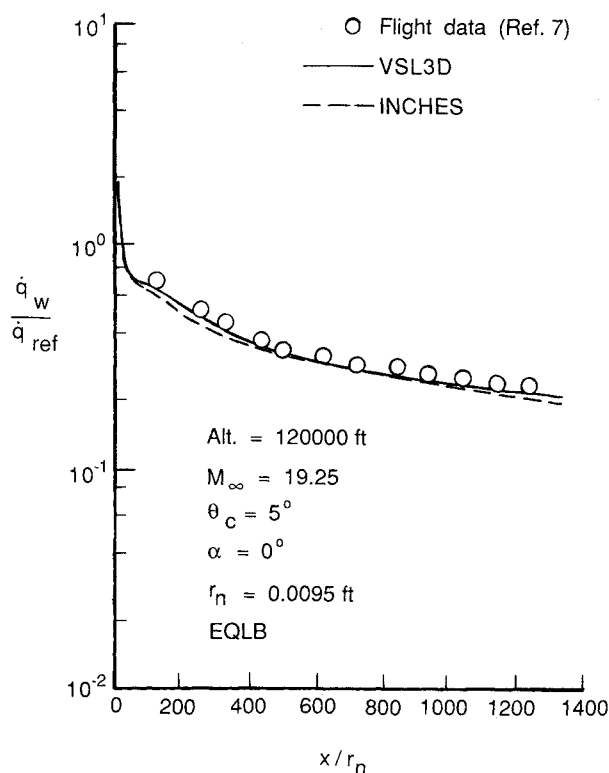


Fig. 2 Comparison of heating predictions with Reentry F data.

made. These results are presented in Fig. 1 for a very long, 5-deg spherically blunted cone at Mach numbers of 15 and 25 and 0-deg angle of attack. The predicted heating-rate distributions using equilibrium air chemistry in both codes are in excellent agreement over the length of the vehicle.

#### Comparison of Predictions with Experimental Data

Figures 3–5 contain comparisons of flight data and heating-rate predictions using the detailed viscous-shock-layer and approximate codes for three Reentry F trajectory points. Equilibrium air chemistry was used in all of the Reentry F calculations. Figure 2 represents data at an altitude of 120,000 ft with a freestream Mach number of 19.4. The flow in this case was laminar over the entire vehicle, and angle of

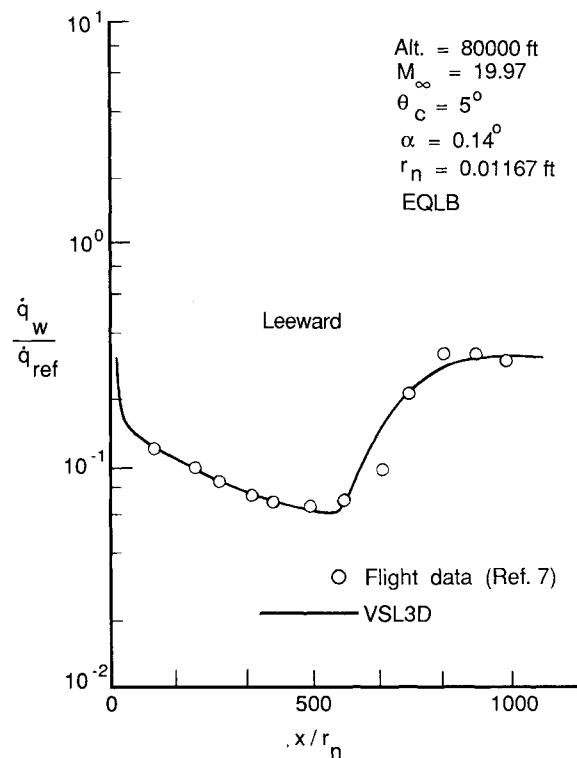


Fig. 3 Comparison of VSL3D prediction with Reentry F data.

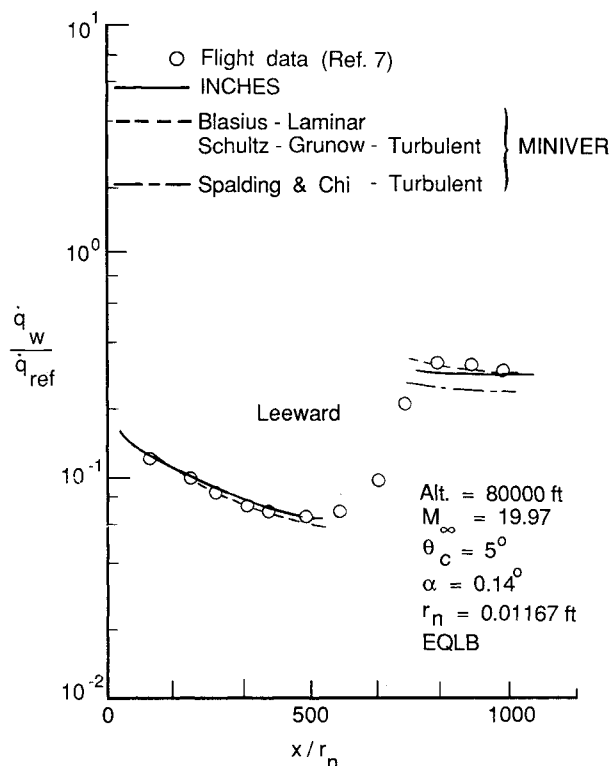


Fig. 4 Comparison of engineering code predictions with Reentry F data.

attack was approximately zero. The comparison between experiment and VSL3D prediction shows agreement within 10% in this case. A heating distribution computed using the INCHES code is in similar agreement with the data and VSL3D result.

Figures 3 and 4 show the experimental data compared with the VSL3D and engineering code predictions, respectively, for

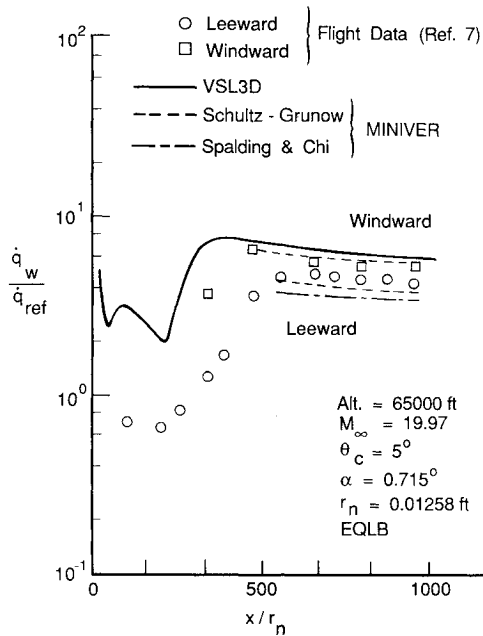


Fig. 5 Comparison of heating predictions with Reentry F data.

trajectory point at 80,000 ft. The Mach number remained near 20 for this case, but a small angle of attack (0.14 deg) existed for the flight vehicle. In the VSL solution, a three-dimensional flowfield was computed, and for the MINIVER code, the equivalent cone approximation was used to account for the pitch. Such a simplifying approximation in the MINIVER solutions is adequate in this case but is not expected to be accurate at larger angles of attack. The data and predictions shown in Figs. 3 and 4 are for the most leeward plane (the primary thermocouple ray). The data show that boundary-layer transition occurred about halfway down the vehicle on the leeward side. For the present calculations, the transition location was taken at the reported distance.<sup>7</sup> In Fig. 3, the overall agreement between heating data and predicted results is excellent except in the transition region. The VSL3D code initially overpredicts the transitional heating, but then underpredicts it as fully turbulent flow is reached. Reasons for this discrepancy have not been investigated.

Figure 4 presents laminar and turbulent heating-rate predictions using the INCHES and MINIVER codes for the same conditions shown in the previous figure. Both engineering codes assume instantaneous transition for this comparison. As shown, the INCHES prediction is in good agreement (within 10%) with both the laminar and fully turbulent data. The laminar heating method in MINIVER also yields results in good agreement with the data. After transition, the results of both turbulent heating methods used in MINIVER are compared with the data. The first, based on the Schultz-Grunow skin-friction relation, is in very good agreement with the data. Conversely, the Spalding and Chi skin-friction relation results in turbulent heating rates 15–20% lower than the data. Similar results have been noted previously.<sup>34</sup>

The last comparison with Reentry F data is shown in Fig. 5. The freestream conditions for this case were at Mach 20 at 65,000 ft, and the angle of attack was 0.715 deg. This figure compares the laminar and turbulent VSL3D solution on the windward plane and the turbulent windward and leeward MINIVER predictions. A leeside heating prediction from VSL3D for the full length of the vehicle was not obtained in this case due to the code "dropping" the solution planes between  $\phi = 135$  and  $180$  deg. The failure of the VSL3D code to compute the leeside flowfield is typical at high angles of attack or for very long bodies at even lower angles of attack.

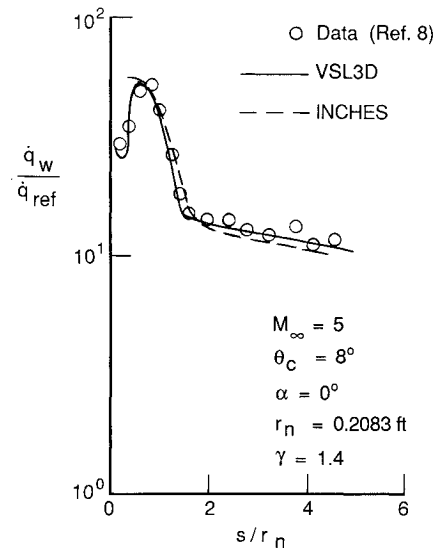


Fig. 6 Comparison of turbulent heating predictions with wind-tunnel data.

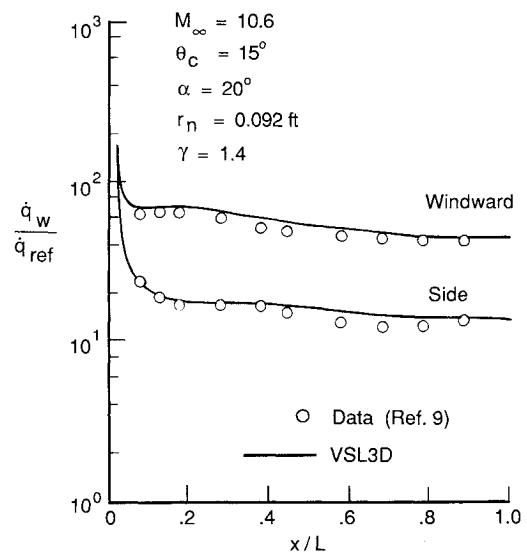


Fig. 7 Comparison of angle-of-attack heating predictions with wind-tunnel data.

The dropping of planes is a limitation of the VSL method and is generally attributed to crossflow separation or to failure in adequately resolving gradients on the leeside. Nevertheless, the entire windward flowfield was computed for this case. An axisymmetric transition location, obtained from the heating measurements on the primary thermocouple ray (leeside), was used in the calculations. The flight data actually indicate transition more forward on the windward ray than on the leeside. Thus, the VSL3D prediction on the windward ray is not comparable with the data in the transition region, but farther downstream the level of turbulent heating compares fairly well (10–12%). Figure 5 also shows the leeward and windward heating predicted with the MINIVER code. The results predicted by the Schultz-Grunow method on the windward and leeward planes are within 10% of the data. A leeside prediction using Spalding and Chi is again 20% lower than the data.

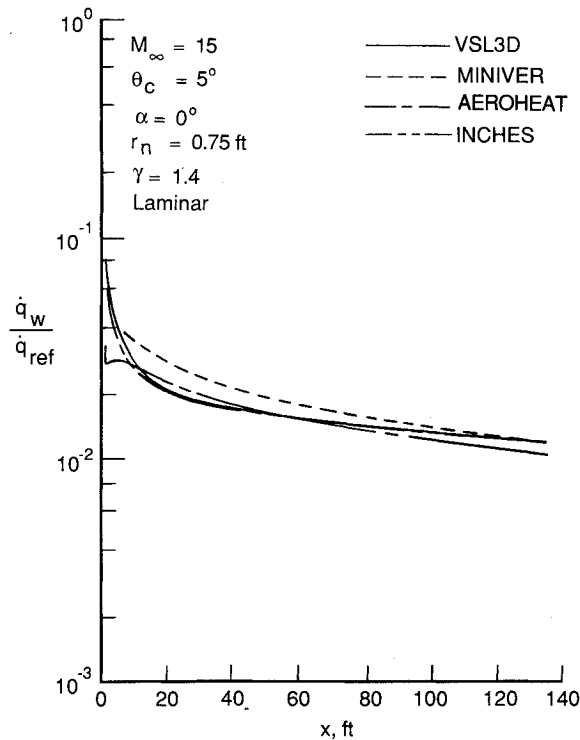


Fig. 8 Comparison of VSL3D and engineering code predictions for laminar heat transfer.

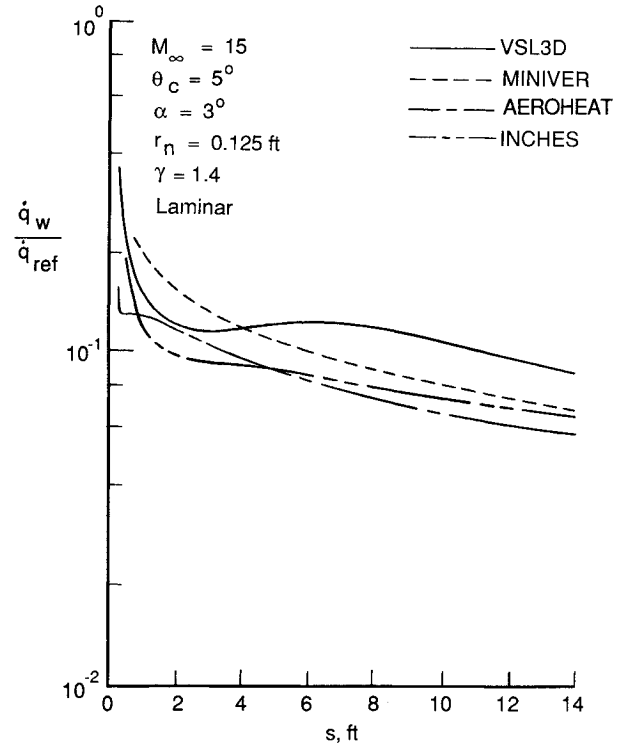


Fig. 10 Comparison of fore-cone laminar heating predictions.

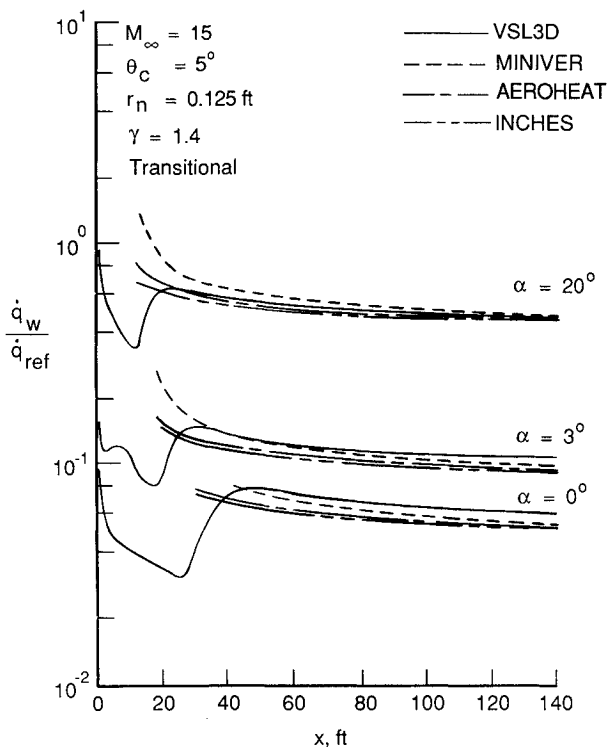


Fig. 9 Comparison of aft-cone turbulent heating predictions.

Additional comparisons of prediction and experiment were made for this study using some of the test results from two wind-tunnel experiments.<sup>8,9</sup> These data were selected to illustrate the effects of turbulent flow and angle of attack, respectively. Conditions for the first case were at Mach 5 and 0-deg angle of attack. The blunt cone half-angle was 8 deg and the body length was 6 nose radii. Natural transition occurred just

downstream of the blunted nosetip and is modeled in the numerical solutions. A comparison of the heating rates predicted with VSL3D and INCHES is presented in Fig. 6 and shows excellent agreement for this blunt-body-dominated flow.

A second comparison of VSL3D prediction with wind-tunnel data is presented in Fig. 7 for a 15-deg sphere cone at 20-deg angle of attack at Mach 10.6. The laminar heating distributions on the windward and side ( $\phi = 90$  deg) meridionals only are shown in Fig. 7, since predictions on the leeside were not obtained. However, this figure still illustrates the good accuracy obtained for the windward side and adds to the confidence level in the angle-of-attack capability of VSL3D.

#### Comparison of VSL3D and Engineering Code Results

Additional comparisons between the engineering codes and VSL3D are presented in this section. Calculations were performed for two 5-deg conical vehicles with nose radii of 0.125 and 0.75 ft at angles of attack of 0, 3, and 20 deg, and some of the results are included herein. Figures 8–10 compare the windward centerline heating rates predicted with the three engineering codes and VSL3D. Figure 8 compares the laminar 0-deg angle-of-attack case for the bluntest vehicle. To simplify the remaining illustrations, and Fig. 9 compares the turbulent afterbody predictions, and Fig. 10 compares the laminar forebody solutions in more detail. For the turbulent calculations, the Schultz-Grunow skin-friction relation in MINIVER was used. The Van Driest<sup>35</sup> skin-friction relation was selected in the AEROHEAT code to compute the heating.

The heating predictions obtained using the engineering methods and VSL3D for the completely laminar flow case at 0-deg angle of attack are generally in fair agreement (Fig. 8). Results from the INCHES code are within 10% of the VSL3D results over the entire length. The levels obtained from AEROHEAT are in good agreement where the pressure overexpansion occurs but are lower than the VSL3D prediction after sharp cone pressure is reached. This can be seen

near the aft end of the vehicle. This method also predicts an unrealistic heating distribution downstream of the sphere-cone tangent point as seen in Fig. 8. The reasons for these discrepancies can be partially attributed to the use of modified Newtonian pressure. Since completion of the present work, Riley et al.<sup>36</sup> have incorporated curve-fit expressions for the pressure into the AEROHEAT code and have obtained better agreement in both the tangent-point region and in regions where sharp cone conditions exist. The MINIVER code in this case yielded heating rates 20% higher than the VSL3D values in regions affected by variable entropy, i.e., the first 35 ft (half the length) of the blunted cone. Elsewhere, the heating levels were within 10% of the VSL3D results. Comparison of the MINIVER heating predictions did not improve when normal shock entropy and modified Newtonian pressure were assumed.

Turbulent heating levels for the smaller nose radius body are shown in Fig. 9 for the three angle-of-attack conditions with the turbulent flow occurring primarily under sharp cone conditions. The general agreement between the engineering codes and VSL3D is good for all the angle-of-attack conditions. The largest differences observed are about 20%, but the overall agreement is between 10 and 15%. Results similar to these were found for the 0.75-ft nose radius body, although the turbulent flow occurs in a region affected by the nose bluntness.

Comparison of heating predictions for the laminar flow regions are shown in Fig. 10 for the 0.125-ft nose radius body at 3- and 20-deg angles of attack. These figures are enlarged views of the fore-cone heating on the present vehicle. At 3-deg angle of attack, discrepancies between the engineering codes and VSL3D laminar results increase, as shown in the figure. The VSL3D prediction exhibits a local maximum in heating near a body location of 7 ft and the maximum is as much as 40% higher than the other predicted values. On the blunter body, this maximum was shifted downstream and occurred beyond the present laminar solutions. This local maximum in heating has been shown in experimental and computational results<sup>9,37</sup> for blunt cones at angle of attack and can also be observed in Fig. 8. Mayne<sup>37</sup> has related this peak to a local maximum in  $|d^2p/d\phi^2|$  and showed that the location of maximum pressure after recompression was slightly downstream of this point. The present VSL solutions also exhibit similar behavior. In the present comparisons, the INCHEs code appears to predict the trend in local maximum but is low in comparison to the VSL3D result. The heating levels from the AEROHEAT code are similar to the INCHEs results but do not exhibit the same trend. Attempts were made in the present study to isolate reasons for the heating discrepancy between the VSL3D, INCHEs, and AEROHEAT codes, and it was concluded that the metrics computed in the engineering codes to describe the streamline spreading for the axisymmetric analog may not be adequate for small angle cones at small angles of attack. Both codes employed the metric definition given by DeJarnette and Davis.<sup>19</sup> Subsequent to this study, Riley et al.<sup>36</sup> have found that the metrics are best computed by using the pressure distribution. Comparisons of AEROHEAT predictions with VSL3D in Ref. 36 show marked improvement and an acceptable heating prediction from AEROHEAT after this modification. The prediction from MINIVER in this case is higher than the other engineering codes, but the slightly better agreement with the VSL result is considered fortuitous. The comparison of predicted heating rates for the small nose radius body at 20-deg angle of attack is also shown in Fig. 10. The VSL solution again shows a local maximum in heating which has moved forward and become of lesser extent with angle of attack and corresponds with the movement of the pressure distribution. Since this effect is more confined in this case, the engineering codes are in better overall agreement with VSL3D than for the lower angle-of-attack case. The overall differences are about 15% with larger disagreement near the heating peak.

**Table 1 Laminar stagnation-point heat transfer at  $M_\infty = 15$ ,  $\gamma = 1.4$**

$r_n$ , ft	VSL3D	$\dot{q}_o$ , $\frac{\text{Btu}}{\text{ft}^2\text{-s}}$	INCHES without viscous effects
		INCHES with viscous effects	
0.125	404.8	390.1	336.8
0.75	163.9	159.2	137.5

Stagnation heating values from VSL3D and INCHEs are compared in Table 1 for the present case. The two sets of heating predictions from INCHEs result from assumptions of edge conditions based on inviscid body streamline calculations or calculations accounting for viscous effects along the stagnation streamline. The results accounting for viscous effects are in excellent agreement with the VSL3D values. The engineering prediction based on inviscid stagnation conditions are typical of boundary-layer methods and are approximately 17% less than the VSL3D results. For decreasing Reynolds number (increasing altitude), these discrepancies will increase. Currently, the thrust of many analyses and design efforts is to account for the lower heating rates associated with nonequilibrium flow and low surface catalysis. However, many of these investigations, in particular those related to the stagnation region, utilize nonequilibrium boundary-layer methods which are not coupled with flowfield solutions. Consequently, the benefits derived by the nonequilibrium heating calculations may be obscured by neglecting effects of the viscous dominated region.

### Concluding Statement

Application of a three-dimensional viscous-shock-layer code (VSL3D) and several approximate "engineering" techniques were demonstrated in this paper. Comparisons of predictions obtained with these methods with Reentry F flight data showed excellent results for both laminar and turbulent flow. The calculations included small angle-of-attack and equilibrium air effects. Results of VSL3D predictions showed excellent agreement with experimental ground test data for turbulent and angle-of-attack conditions and also with corresponding results of a parabolized Navier-Stokes code.

Comparisons of engineering codes and VSL3D results were also made to evaluate the applicability of the approximate methods. The predicted results showed generally good agreement but illustrated some deficiencies in the approximate techniques. These results can be summarized as follows:

- 1) Windward centerline turbulent heating rates predicted by the engineering and VSL3D codes were in good agreement over the range of bluntness and angle of attack considered.
- 2) Laminar heating distributions computed with the MINIVER code were 20–30% higher than other predictions in regions affected by variable entropy. These results indicate that the method may be unsuitable for studies where bluntness influences a significant part of the flowfield.
- 3) Laminar heating rates predicted with the INCHEs code were in good agreement with the VSL3D results for the case at 0-deg angle of attack. However, at small angles of attack, the agreement on the windward centerline deteriorated and large differences (as much as 40%) were noted. Similar results were obtained with the AEROHEAT code. The discrepancies are due to inaccuracies in the metric expressions used in the engineering codes to describe the streamline spreading effect for angle-of-attack conditions. Subsequent modifications<sup>36</sup> to AEROHEAT have improved the code's ability to predict slender cone heating.
- 4) Approximate heating methods or boundary-layer codes should be coupled with a flowfield procedure to account for viscous effects in the stagnation region at low Reynolds number conditions.

## References

- <sup>1</sup>Engel, C. D. and Praharaj, S. C., "MINIVER Upgrade for the AVID System. Vol. I: LANMIN User's Manual," NASA CR-172212, Aug. 1982.
- <sup>2</sup>DeJarnette, F. R. and Hamilton, H. H., II, "Aerodynamic Heating on 3-D Bodies Including the Effect of Entropy-Layer Swallowing," *Journal of Spacecraft and Rockets*, Vol. 12, Jan. 1975, pp. 5-12.
- <sup>3</sup>Zoby, E. V. and Simmonds, A. L., "Engineering Flowfield Method with Angle-of-Attack Applications," *Journal of Spacecraft and Rockets*, Vol. 22, July-Aug. 1985, pp. 398-404.
- <sup>4</sup>Murray, A. L. and Lewis, C. H., "Hypersonic Three-Dimensional Viscous Shock Layer Flows Over Blunt Bodies," *AIAA Journal*, Vol. 16, Dec. 1978, pp. 1279-1286.
- <sup>5</sup>Thareja, R. R., Szema, K. Y., and Lewis, C. H., "Chemical Equilibrium Laminar or Turbulent Three-Dimensional Viscous Shock-Layer Flows," *Journal of Spacecraft and Rockets*, Vol. 20, Sept.-Oct. 1983, pp. 454-460.
- <sup>6</sup>Swaminathan, S., Kim, M. D., and Lewis, C. H., "Three-Dimensional Nonequilibrium Viscous Shock-Layer Flows Over Complex Geometries," AIAA Paper 83-0212, Jan. 1983.
- <sup>7</sup>Stainback, P. C., Johnson, C. B., Boney, L. B., and Wicker, K. C., "Comparison of Theoretical Predictions and Heat-Transfer Measurements for a Flight Experiment at Mach 20 (Reentry F)," NASA TM X-2560, 1972.
- <sup>8</sup>Jackson, M.D. and Baker, D.L., "Passive Nosedip Technology (PANT) Program. Vol. 3. Surface Roughness Effects. Part 1: Experimental Data," Acurex Corp., SAMSO-TR-74-86-VOL-3-PT-1, Jan. 1974.
- <sup>9</sup>Cleary, J. W., "Effects of Angle of Attack and Bluntness on the Shock-Layer Properties of a 15° Cone at a Mach Number of 10.6," NASA TN D-4909, Nov. 1968.
- <sup>10</sup>Gnoffo, P. A., "Hypersonic Flows Over Biconics Using a Variable-Effective-Gamma, Parabolized Navier-Stokes Code," AIAA Paper 83-166, July 1983.
- <sup>11</sup>Wilhite, A. W., "The Aerospace Vehicle Interactive Design System," AIAA Paper 81-233, Jan. 1981.
- <sup>12</sup>Fay, J. A. and Riddell, F. R., "Theory of Stagnation-Point Heat Transfer in Dissociated Air," *Journal of Aeronautical Sciences*, Vol. 25, Feb. 1958, pp. 73-85, 121.
- <sup>13</sup>Schlichting, H., *Boundary-Layer Theory*, 4th ed., McGraw-Hill, New York, 1960, Chap. 6.
- <sup>14</sup>Eckert, E. R. G., "Survey on Heat Transfer at High Speeds," U.S. Air Force, ARL-189, Dec. 1961.
- <sup>15</sup>Schultz-Grunow, F., "A New Resistance Law for Smooth Plates," *Luftfahrt Forsch.*, Vol. 17, 1940, pp. 239-246; (translation) NACA TM 986, 1941.
- <sup>16</sup>Spalding, D. B. and Chi, S.W., "The Drag of a Compressible Turbulent Boundary Layer on a Smooth Flat Plate With and Without Heat Transfer," *Journal of Fluids Mechanics*, Vol. 18, Pt. 1, Jan. 1964, pp. 117-143.
- <sup>17</sup>Mangler, W., "Boundary Layers with Symmetrical Airflow About Bodies of Revolution," Goodyear Aircraft Corporation Report R-30-18 (Translation), 1946.
- <sup>18</sup>Cooke, J. C., "An Axially Symmetric Analog for General Three-dimensional Boundary Layers," British A.R.C., R&M No. 3200, 1961.
- <sup>19</sup>DeJarnette, F. R. and Davis, R. M., "A Simplified Method for Calculating Laminar Heat Transfer Over Bodies at an Angle of Attack," NASA TN D-4720, 1968.
- <sup>20</sup>Hamilton, H. H., II, "Calculation of Laminar Heating Rates on Three-Dimensional Configurations Using the Axisymmetric Analogue," NASA TP 1698, Sept. 1980.
- <sup>21</sup>DeJarnette, F. F. and Hamilton, H. H., II, "Inviscid Surface Streamline and Heat Transfer on Shuttle-Type Configurations," *Journal of Spacecraft and Rockets*, Vol. 10, No. 6, May 1973, pp. 314-321.
- <sup>22</sup>Maslen, S. H., "Inviscid Hypersonic Flow Past Smooth Symmetric Bodies," *AIAA Journal*, Vol. 2, June 1964, pp. 1055-1061.
- <sup>23</sup>Cohen, N. B., "Boundary-Layer Similar Solutions and Correlation Equations for Laminar Heat-Transfer Distribution in Equilibrium Air at Velocities Up to 41,000 Feet Per Second," NASA TR R-118, 1961.
- <sup>24</sup>Maslen, S. H., "Axisymmetric Hypersonic Flow," NASA CR-2123, 1972.
- <sup>25</sup>Johnson, C. B. and Bushnell, D. M., "Power-Law Velocity-Profile-Exponent Variation With Reynolds Number, Wall Cooling, and Mach Number in a Turbulent Boundary Layer," NASA TN D-5753, April 1970.
- <sup>26</sup>Davis, R. T., "Numerical Solution of the Hypersonic Viscous Shock-Layer Equations," *AIAA Journal*, Vol. 8, Dec. 1970, pp. 2152-2156.
- <sup>27</sup>Cebeci, T., "Behavior of Turbulent Flow Near a Porous Wall with Pressure Gradient," *AIAA Journal*, Vol. 8, Dec. 1970, pp. 2152-2156.
- <sup>28</sup>Adams, J. C., Jr., "Analysis of the Three-Dimensional Compressible Turbulent Boundary Layer on a Sharp Cone at Incidence in Supersonic and Hypersonic Flow," Arnold Engineering Development Center, Arnold Air Force Station, TN, AEDC-TR-72-66, June 1972.
- <sup>29</sup>Clauser, F. H., "The Turbulent Boundary Layer," Vol. IV of *Advances in Applied Mechanics*, edited by H. L. Dryden and T. von Karman, Academic Press, New York, 1956, pp. 1-51.
- <sup>30</sup>Klebanoff, P. S., "Characteristics of Turbulence in a Boundary Layer with Zero Pressure Gradient," NASA Rept. 1247, 1955.
- <sup>31</sup>Dhawan, S. and Narashima, R., "Some Properties of Boundary-Layer Flow During Transition from Laminar to Turbulent Motion," *Journal of Fluid Mechanics*, Vol. 3, Pt. 4, Jan. 1958, pp. 418-436.
- <sup>32</sup>Hansen, C. F., "Approximations for the Thermodynamic and Transport Properties of High-Temperature Air," NASA TR R-50, 1959.
- <sup>33</sup>Wright, R. L. and Zoby, E. V., "Flight Boundary-Layer Transition Measurements on a Slender Cone at Mach 20," AIAA Paper 77-719, June 1977.
- <sup>34</sup>Zoby, E. V. and Graves, R. A., "Comparison of Results from Three Prediction Methods with Turbulent Heating Data from Wind-Tunnel and Free-Flight Tests," NASA TM X-2390, Sept. 1971.
- <sup>35</sup>Van Driest, E. R., "Turbulent Boundary Layers in Compressible Fluids," *Journal of Aerospace Sciences*, Vol. 18, March 1956, pp. 145-160, 216.
- <sup>36</sup>Riley, C. J., DeJarnette, F. R., and Zoby, E. V., "Effects of Surface Pressures and Streamline Metrics on the Calculation of Laminar Heating Rates," AIAA Paper 88-2708, June 1988.
- <sup>37</sup>Mayne, A. W., "Calculation of the Boundary-Layer Flow in the Windward Symmetry Plane of a Spherically Blunted Axisymmetric Body at Angle of Attack, Including Streamline-Swallowing Effects," Arnold Engineering Development Center, Arnold Air Force Station, TN, AEDC-TR-73-166, Oct. 1973.